ACS APPLIED MATERIALS & INTERFACES

Letter

www.acsami.org

# Controlling Bandgap of Rippled Hexagonal Boron Nitride Membranes via Plasma Treatment

H. X. Zhang[†,‡] and P. X. Feng*[,†]

[†]Institute for Functional Nanomaterials and Department of Physics, University of Puerto Rico, Rio Piedras Campus, P.O. Box 23343, San Juan, PR 00925, Puerto Rico

[‡]Materials Science and Technology Division, Oak Ridge National Laboratory, P.O. Box 2008, MS-6087, Oak Ridge, Tennessee 37831, United States

**ABSTRACT:** Few-layer rippled hexagonal boron nitride (h-BN) membranes were processed with hydrogen plasma, which exhibit distinct and pronounced changes in its electronic properties after the plasma treatment. The bandgaps of the h-BN membrane reduced from ~5.6 eV at 0 s to ~4.25 eV at 250s, which is a signature of transition from the insulating to the semiconductive regime. It typically required 250 s of plasma treatment to reach the saturation. It illustrates that two-dimensional material with engineered electronic properties can be created by attaching other atoms or molecules.

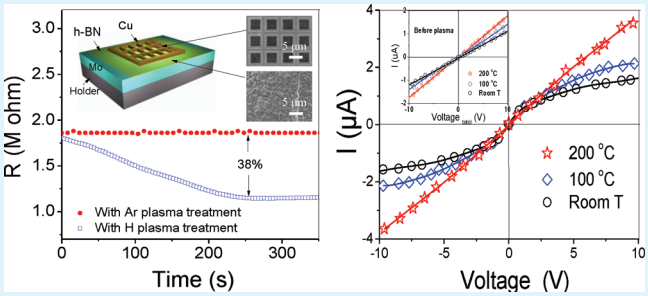


**KEYWORDS:** *h-BN membrane, ripples, bandgap, hydrogenation, plasma, TEM*

Atomically thin hexagonal boron nitride (h-BN) membrane is considered the thinnest possible two-dimensional crystal with slightly ionic bonds, which exhibits notable electronic, thermal, chemical, and mechanical properties including high mechanical stiffness and strength.[1−5] A wealth of science and applications are expected from single-layer and few-layer h-BN membrane.[6−8] For example, having a lattice constant nearly same as that of graphene suggests a joint use of h-BN membranes in composite devices.[9] These motivates considering h-BN membranes for next-generation electronic devices.[10−16] However, the wide bandgap of h-BN is a serious obstacle for its application in electronics, despite its high thermal and chemical stabilities.[17,18]

In present work, we report the bandgap control of rippled h-BN membranes by hydrogen plasma modification. Dramatic changes have been observed in transport properties in h-BN membranes, as evidenced by electronical measurements and transmission electron microscopy (TEM).

h-BN membranes were produced by using supershort-pulse laser produced plasma deposition techniques. An ArF Lambda Physik 1000 excimer laser (193 nm, ~20−30 ns, and 10 Hz repetition rate, and <300 mJ pulse energy) was used to irradiate the BN target under high vacuum. The h-BN source was provided by the commercial BN target (99.99% Pure 2.00″ Dia. × 0.125″ Tk., Density: 1.94 g/cm$^3$) from Kurt J. Lesker Company. The laser beam, focused with a 30 cm focal length fused silica lens, was incident at 45 degrees relative to the target surface. The use of the long focal length fused lens is to effectively control the laser- produced plasma beams. The power density of the laser on the target was controlled at 1.1 × 10$^8$ W/cm$^2$ per pulse. The target was rotated at ~200 rpm. The Mo wafers were placed 4 cm away from the target. Prior to laser irradiation, the Mo wafers were polished and rinsed in acetone and methanol in sequence. The duration for each deposition was 30 min. The detailed description of growth of h-BN membranes can be found in our previous publication.[19,20]

Considering h-BN is wide bandgap material, a special measurement setup was made to ensure the electrical signal in the detectable range, which is shown in Figure 1a. A mesh-type copper pad, which serves as electrode, was used to contact to the h-BN membranes for the purpose of facilitating plasma treatment. The effective resistance between the two electrodes is only from the h-BN membrane, which means the electron will vertically go through h-BN membranes when the voltage is applied between electrodes. It should be mentioned that the electrical signal from the in-plane h-BN membrane is out of our detectable range.

Before plasma treatment, h-BN membranes were annealed in ultrahigh purity argon at 120 °C for 90 min and transferred under argon to the characterization chamber. We first annealed all samples at 300 °C in an argon atmosphere for 2 h in order to remove major contamination. Then, the samples were exposed to a cold plasma. A low-pressure (10 Pa) hydrogen/argon mixture (10% $H_2$) was used with dc plasma ignited between two electrodes. The samples were kept 4 cm away from the discharge zone to minimize any possible damage by energetic ions. Electrical characteristics of the samples were measured in situ during plasma treatment.

Typical changes induced by the hydrogen plasma treatment in electronic properties of h-BN membranes are illustrated in

**Received:** October 18, 2011
**Accepted:** December 27, 2011
**Published:** December 27, 2011

   dx.doi.org/10.1021/am201435z | *ACS Appl. Mater. Interfaces* 2012, 4, 30−33

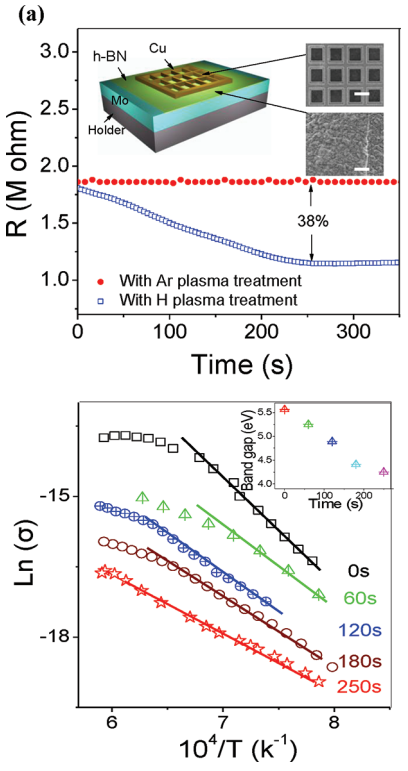


**Figure 1.** (a) In situ measurement of resistance of the h-BN membranes with hydrogen plasma treatment as a function of time. Inset: illustration of the setup for measuring the electronic properties of h-BN membranes. (b) Logarithm of the electric conductivity of h-BN membranes plotted against the reciprocal temperature during hydrogen plasma treatment. The scale bars in the inset of a are 5 $\mu$m.

Figure 1. Before plasma exposure, the contact resistance of the h-BN membranes was about 1.8 M ohm. As a reference, h-BN membranes were exposed to pure Ar plasma. The h-BN membranes only showed very little change in their resistance. This behavior significantly changed after h-BN membranes were treated with atomic hydrogen plasma, which exhibits a strong time dependence of its resistivity during hydrogen plasma treatment. The resistance of h-BN membranes decreased by 38%, as shown in Figure 1a. It typically required 250 s of plasma treatment to reach the saturation in measured characteristics, showing that h-BN membranes were processed with hydrogen plasma step by step.

Figure 1b show the logarithm of the electric conductivity versus the reciprocal temperature at hydrogen plasma treatment 0, 60, 120, 180, and 250 s, respectively. Namely, the cumulative electrical conduction ($\sigma$) of a semiconducting substance is determined by the following equation:[13]

$$\sigma = \sigma_o T^{3/2} \exp(-E_g/2kT) + \sigma'_o \exp(-\Delta E/kT) \quad (1)$$

where $\Delta E$ is the ionization energy of the impurity level, $k$ the Boltzmann's constant, while $\sigma$ and $\sigma'$ are constants. The two terms in the eq 1 correspond to the intrinsic and extrinsic conduction mechanism, respectively.[13,21] The impurity and or the defect content affects the concentration of carriers, which is determined by the intrinsic properties of the pure semiconductor crystal.[13,21] In the intrinsic region, the temperature dependence of the conductivity is dominated by an exponential factor

$$\sigma \propto \exp(-E_g/2k_BT) \quad (2)$$

Therefore, the plot of log $\sigma$ versus $1/T$ gives a straight line in the intrinsic region, and the magnitude of the slope gives the energy gap.[21] The inset in Figure 2b shows the bandgaps of h-BN membranes processed at 0, 60, 120, 180, and 250 s, respectively. Following the time, the bandgaps of h-BN membranes decreased from ~5.6 eV at 0 s to 4.25 eV at 250 s, which is a signature of transition from insulating to semiconductive regime.

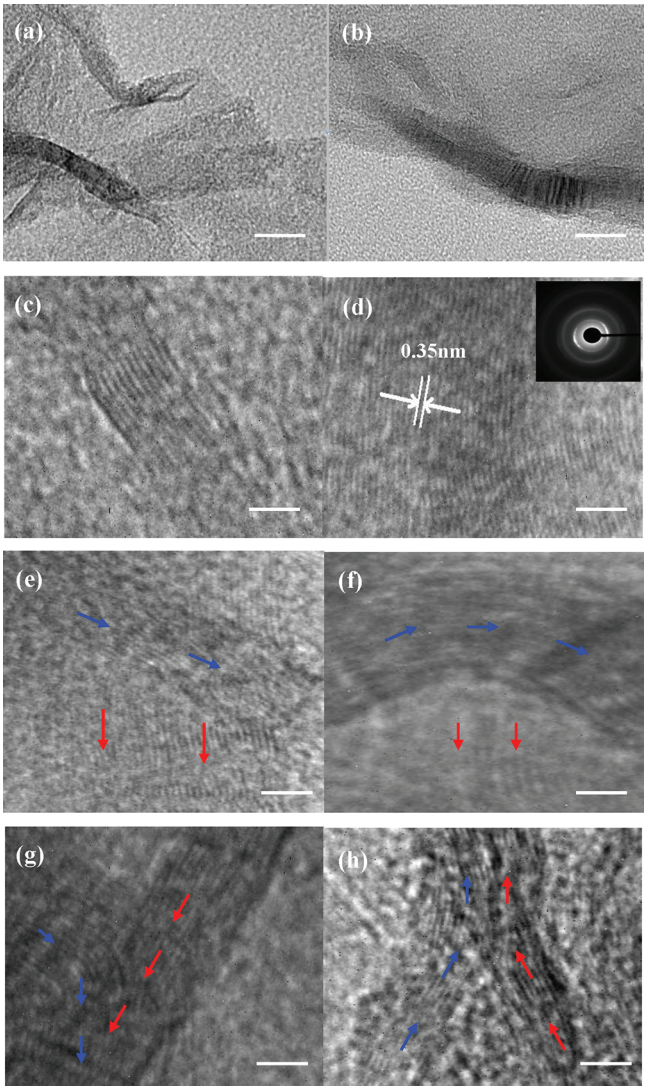


**Figure 2.** (a) TEM Image of an area with several ripples. (b) Magnified image of ripples. (c) One-dimensional ripples. (d) Large-area individual structure consisting of one-dimensional ripples. The insert is the corresponding SEAD of the regions. (e–h) Cases where two structures of ripples are combined could be caused by roughness and grain boundaries present on the surface, or drying process and shrinkage associated with the film preparation. The scale bar of (a) is 50 nm, (b) is 20 nm, and (c–h) are 2 nm.

To observe the nanoscale morphology of h-BN membranes, h-BN membrane samples were scathed off and transferred to the grids for TEM measurement by using optical microscopy. TEM image in Figure 2a suggests that h-BN membranes are not microscopically flat but rippled. The ripple structure with one direction is shown in Figure 2c. Large-area ripples with one


dx.doi.org/10.1021/am201435z | ACS Appl. Mater. Interfaces 2012, 4, 30–33

direction is shown in Figure 2d. The selected area electron diffraction (SAED) image in the insert of Figure 2d shows typical disorder structures in h-BN membranes.[22] It should be mentioned that the clear lattice fringes were only observed in certain areas, which may explain the poor crystallinity of h-BN membranes shown in SAED and Raman spectra. Unusual rippled structures were observed shown in Figure 3(e–h).

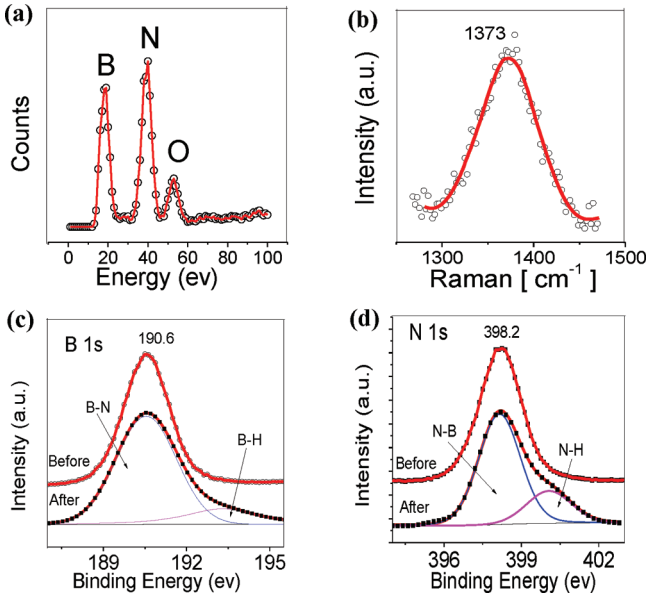


**Figure 3.** (a) Typical EDS analysis of hydrogen plasma-treated h-BN membranes. (b) Raman spectrum of hydrogen plasma-treated h-BN membranes recorded at room temperature, exited by 514 nm laser. Their main Raman peak near 1373 $cm^{-1}$. The Lorenz curve (red solid) was used here to fit the peak. (c–d) XPS spectra of B and N 1s core levels before and after hydrogen plasma treatment. The spectral data are fitting by Gaussian curves (red solid).

Associated with the widths, density or directions of the ripples, we observe various cases where ripples with different directions are combined, which could be caused by roughness and grain boundaries present on the surface, or drying process and shrinkage associated with the membrane preparation. (i) Superposition of ripples consisting of two bundles of straight ripples. (ii) One bundle of ripples cross over one bundle of curved ripples. (iii) Straight ripples overlap with circle-shaped ripples. (iv) Two ripples merge into one. It is not yet clear how the superposition negotiates its bonding with the h-BN membranes; presumably all the ripples are held in place simply by van der Waals bonding with atoms in the underlying h-BN membranes, and thus it would constitute a superposition of ripples.

Theoretical calculations have indicated that h-BN membranes exhibit diverse electronic properties after hydrogenation.[17] The hydrogenated BN sheet has a band gap between the bonding N $2p_x$ and $2p_y$ orbitals in the plane and the antibonding N $2p_z$ and $H_N$ 1s orbitals out of the plane.[23] Thus, the hydrogenation changes the band character of the BN sheet, which leads to a smaller band gap than for the pristine one.[23] For the case of h-BN membranes on a substrate, we can exclude the possibility of double-sided hydrogenation and confirm the single-sided hydrogenation. Single-sided hydrogenation of flat h-BN membranes would create a material that is thermodynamically unstable, however, rippled structures would facilitate single-sided hydrogenation.[24,25]Because the lattice is already deformed in the direction that favors $sp^3$ bonding on a convex surface, which lowers the total energy.[24,25] Single-sided hydrogenation becomes energetically favorable for ripples observed experimentally.[24,25]

Energy dispersive X-ray spectroscopy (EDS) was employed to quantitatively analyze the chemical composition of the hydrogen plasma-treated h-BN membranes. The typical EDS spectrum of the hydrogen plasma-treated h-BN membranes is shown in Figure 3a. Technically, the hydrogen plasma-treated h-BN membranes mainly consist of Boron and Nitrogen. A small amount of oxygen was also detected, which possibly derived from the residual air in the chamber and oxygen adsorption during the transport of the samples from the growth chamber to the spectrometer.

Raman scattering spectra of the hydrogen plasma-treated h-BN membranes were also obtained at room temperature by using a triple monochomator (ISA J-Y Model T64000) with an excitation wavelength of 514 nm ($Ar^+$ ion laser). The microscope was used for focusing the laser beam onto the surface of samples. The dominant peak located at 1373 $cm^{-1}$ is attributed to the B–N vibrational mode ($E_{2g}$) shown in Figure 3b. However, the $E_{2g}$ mode of hydrogen plasma-treated h-BN membranes shifts to a higher frequency compared with that of the untreated h-BN,[19,26] which is probably caused by an increase of stress during the plasma treatment.

X-ray photoelectron spectroscopy (XPS), which is a quantitative spectroscopic technique for surface characterization, was used to investigate the composition of BN membranes before and after plasma treatment. The XPS spectra of the hydrogen plasma-treated h-BN membranes are presented in Figure 3c–d. The hydrogen plasma-treated h-BN membranes present a B 1s-core level at 190.6 eV and the N 1s peak is located at 398.2 eV, which is close to the reported position of h-BN.[26] However, the plasma-treated h-BN show broader features than pure h-BN membranes. On the basis of the literature,[26–28] the N 1s and B 1s core of hydrogen plasma-treated h-BN membrane was deconvoluted into two components, shown in Figure 3c–d.

Figure 4 shows the I–V characteristics of the hydrogen plasma-treated h-BN membranes as a function of applied voltage. They have exhibited strongly nonlinear behavior at

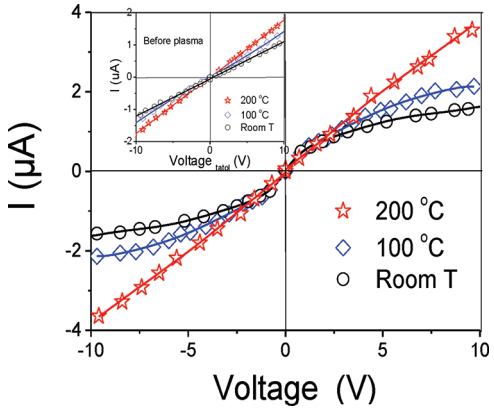


**Figure 4.** *I–V* characteristics of a hydrogen plasma-treated h-BN membranes measured at room temperature, 100 and 200 °C, respectively. Inset: Temperature dependence of the *I–V* characteristics before plasma. From bottom to top: $T$ = 200 °C, 100 °C, and room temperature.


dx.doi.org/10.1021/am201435z | ACS Appl. Mater. Interfaces 2012, 4, 30–33

room temperature after plasma treatment. The nonlinearity of the I−V curves in this system is probably due to the dipole formation at the interface, perturbation of the h-BN membranes beneath the metal, reaction of the metal or h-BN membranes with unwanted impurities at the interface.[29−32] The level of nonlinearity varies with temperature, and the curves become practically linear at 200 °C, which is probably caused by the desorption of hydrogen atoms at higher temperature, leading to recover of h-BN membranes. The inset shows the I−V characteristics of untreated h-BN membranes, all of which have linear behaviors and little change can be observed with increasing temperature.

In conclusion, few-layer rippled h-BN membranes exhibit distinct and pronounced changes in its electronic properties after atomic hydrogen plasma treatment. The resistance R of the h-BN membranes drops by 38% of magnitude with the increasing hydrogen plasma exposing time. It typically required 250 s of plasma treatment to reach the saturation in measured characteristics, which showed that h-BN membranes were processed with plasma step by step. Following the time, the bandgaps of h-BN membranes decreased from ∼5.6 eV at 0 s to ∼4.25 eV at 250s, which is a signature of transition from the insulating to the semiconductive regime. Our results show that adjusting electronic properties of h-BN membranes using molecular engineering is possible.

## AUTHOR INFORMATION

**Corresponding Author**
*E-mail: p.feng@upr.edu.

## ACKNOWLEDGMENTS

This work was supported by NSF/DMR (0706147), and IFN Fellowship. We also thank the National Science Foundation of China (Grant No. 20921004).We would like to thank Mr. Oscar for assistance of TEM measurements, and Mr. Josuel for SEM measurements.

## REFERENCES

(1) Kubota, Y.; Watanabe, K.; Tsuda, O.; Taniguchi, T. *Science* **2007**, *317*, 932.
(2) Lin, Y.; Williams, T. V.; Connell, J. W. *J. Phys. Chem. Lett.* **2010**, *1*, 277.
(3) Watanabe, K.; Taniguchi, T.; Kanda, H. *Nat. Mater.* **2004**, *3*, 404.
(4) Chopra, N. G.; Luyken, R.; Cherrey, K; Crespi, V. H.; Cohen, M. L.; Louie, S. G.; Zettl, A. *Science* **1995**, *269*, 966.
(5) Rubio, A.; Corkill, J. L.; Cohen, M. L. *Phys. Rev. B* **1994**, *49*, 5081.
(6) Alem, N.; Erni, R.; Kisielowski, C.; Rossell, M. D.; Gannett, W.; Zettl, A. *Phys. Rev. B* **2009**, *80*, 155425.
(7) Meyer, J. C.; Chuvilin, A.; Algara-Siller, G. *Nano Lett.* **2009**, *9*, 2683.
(8) Taniguchi, T.; Watanabe, K.; Koizumi, S. *Phys. Status Solidi A* **2004**, *201*, 2573.
(9) Suenaga, K.; Colliex, C.; Demoncy, N.; Loiseau, A.; Pascard, H.; Willaime, F. *Science* **1997**, *278*, 653.
(10) Kawasaki, T.; Ichimura, T.; Kishimoto, H.; Akbar, A. A.; Ogawa, T.; Sshima, C. *Surf. Rev. Lett.* **2002**, *9*, 1459 (2002).
(11) Giovannetti, G.; Khomyakov, P. A.; Brocks, G.; Kelly, P. J.; Van den Brink, J. *Phys. Rev. B* **2007**, *76*, 073103.
(12) Yuge, K. *Phys. Rev. B* **2009**, *79*, 144109.
(13) Carpenter, L. G.; Kirby, P. J. *J. Phys. D: Appl. Phys.* **1982**, *15*, 1143.
(14) Blasé, X.; Rubio, A.; Louie, S. G.; Cohen, M. L. *Europhys. Lett.* **1994**, *28*, 335.
(15) Mohana, A. L.; Tanur, A. E.; Walker, G. C. *Int. J. Hydrogen Energy* **2010**, *35*, 4138.
(16) Giannis, M.; Froudakis, G. E. *Catal. Today* **2007**, *120*, 341.
(17) Wei, C.; Li, Y. F.; Yu, G. T.; Li, C. Z.; Zhang, S. B.; Zhou, Z.; Chen, Z. *J. Am. Chem. Soc.* **2010**, *132*, 1699.
(18) Tang, S.; Cao, Z. *Chem. Phys. Lett.* **2010**, *488*, 67.
(19) Zhang, H. X.; Sajjad, M.; Feng, P. X. *Proc. MRS 2010 Spring Meeting* **2010**, No. 1259-S14-10, DOI: 10.1557/PROC-1259-S14-10.
(20) Sajjad, M.; Zhang, H. X.; Peng, X. Y.; Feng, P. X. *Phys. Scr.* **2011**, *83*, 065601.
(21) Pejova, B.; Grozdanov, I.; Taunsevski, A. *Mater. Chem. Phys.* **2004**, *83*, 245.
(22) Babonneau, D.; Jaouen, M.; Denanot, M. F.; Guerin, P.; Petroff, F. *Appl. Phys. Lett.* **2003**, *82*, 3056.
(23) Wang, Y. L. *Phys. Status Solidi RRL* **2010**, *4*, 34.
(24) Elias, D. C.; Nair, R. R.; Mohiuddin, T. M. G.; Morozov, S. V.; Blake, P.; Halsall, M. P.; Ferrari, A. C.; Boukhvalov, D. W.; Katsnelson, M. L.; Geim, A. K.; Novoselov, K. S. *Science* **2009**, *323*, 610.
(25) Boukhvalov, D. W.; Katsnelson, M. I. *J. Phys. Chem. C* **2009**, *113*, 14176.
(26) Song, L.; Ci, L.; Lu, H.; Sorokin, P. B.; Jin, C.; Ni, J.; Kvashnin, A. G.; Kvashinin, D. G.; Lou, J.; Yakobson, B. I.; Ajavan, P. M. *Nano Lett.* **2010**, *10*, 3209.
(27) Sainsbury, T.; Ikuno, T.; Okawa, D.; Pacile, D.; Frechet, J. M. J.; Zettl, A. *J. Phys. Chem. C* **2007**, *111*, 12992.
(28) Chen, X.; Gao, X. P.; Zhang, H.; Zhou, Z.; Hu, W. K.; Pan, G. L.; Zhu, H. Y.; Yan, T. Y.; Song, D. Y. *J. Phys. Chem. B* **2005**, *109*, 11525.
(29) Tan, Y. W.; Zhang, Y.; Stormer, H. L.; Kim, P. *Eur. Phys. J. Spec. Top.* **2007**, *148*, 15.
(30) Barone, V.; Hod, O.; Scuseria, G. E. *Nano Lett.* **2006**, *6*, 2748.
(31) Han, M. Y.; Ozyilmaz, B.; Zhang, Y.; Kim, P. *Phys. Rev. Lett.* **2007**, *98*, 206805.
(32) Ozyilmaz, B.; Jarillo-Herrero, P.; Efetov, D.; Kim, P. *Appl. Phys. Lett.* **2007**, *91*, 192107.